

Buffet Load Alleviation System for Advanced Commercial Aircraft

Sheharyar Malik, Sergio Ricci, Daniele Monti and Luca Riccobene

Abstract— This paper presents the active control scheme for buffet load attenuation on the wings of advanced commercial aircraft prototype, built under (3AS) European project in Politecnico di Milano. Finite element commercial software, MSC/NASTRAN provided the analytical model of the forward swept wing named as X-DIA. In house software, MASSA, provided the aerodynamic and structural coupling to formulate the Aeroservoelastic model, it excited the structural modes of the wing with buffeting loads, applied as input to the model. Active control scheme has been developed to suppress the excited structural vibrations in the bandwidth range of four control surfaces located on the wing: first and second order algorithms with variable step size were used to minimize the objective function based on the controllability and observability of the system. Dedicated robustness analysis has been performed numerically and experimentally for the uncertainties in the actuators system and accelerometers located on the wing. Numerical investigation on the buffet load attenuation system was validated and supported by dedicated wind-tunnel test campaign at De Ponte wind-tunnel, Politecnico Di Milano. The results demonstrated the considerable attenuation of the buffet loads and effectiveness of the proposed system.

Keywords— buffeting, heuristic, static output feedback control, aeroelastic.

I. INTRODUCTION

THE demand of the industry for high performance, light weight and fuel efficient commercial aircrafts is often met by reducing the weight of the fuselage and wings of the aircraft. Aircrafts operating at high turn rates produce vortices from the aircraft's fore-body resulting in buffeting loads.

Manuscript received April 9, 2018. This work was supported in part by the European Commission under TIVANO project.

S. M. Author is with the Department of Aerospace Science and Technology, Politecnico di Milano, Milan, Italy. (corresponding author to provide phone: +39-02-2399-8085; fax: +39-02-2399-8085; e-mail: sheharyar.malik@polimi.it).

S. R. Author is with the Department of Aerospace Science and Technology, Politecnico di Milano, Milan, Italy. (e-mail: sergio.ricci@polimi.it).

D. M. Author is with the Structural Dynamics Group, LEONARDO Aerospace Company, Aircraft Division, Venegono Superior, Italy. (e-mail: daniele.monti@leonardocompany.it).

L. R. Author is with the Department of Aerospace Science and Technology, Politecnico di Milano, Milan, Italy. (e-mail: luca.riccobene@polimi.it).

Immersed in the zone of these dynamic loads, lightweight wings with resonant modes at low frequencies become more vulnerable to the vortices, coupling together to produce vibrations in the wing. If these structural vibrations are unaddressed, it does not only limit the flight envelope but it also leads to trigger the fatigue cracks, which require additional repairs or replacement [1, 2].

Many possibilities have been investigated in the past researches to attenuate the buffet loads. These include active and passive techniques based on structural dynamic and aerodynamic methods [3]. Notable passive aerodynamic technique includes leading edge extension on the F/A-18 aircraft. Tangential leading-edge blowing is used as active aerodynamic technique [4]. Passive structural technique such as adding reinforcement to stiffen the structure are commonly used to avoid structural vibrations due to buffet loads. Fortunately, often these structural vibrations fall in the operating bandwidth of the actuators, which can be used to attenuate the buffeting loads by using the active structural technique. In [5, 6], authors have developed the LQG (Linear Quadratic Gaussian) controller to attenuate the buffet loads on the vertical tail of the aircraft. Piezoelectric actuators glued to the surface of the vertical fin are also used to compare it with the results of using rudder as actuator. All the above-mentioned researches suggested the attenuation of vibrations to some extent, measured as either in power spectral density, frequency response or in root-mean-square (rms) value. In [7], method based on static output feedback controller based on second order quadratic formulation is presented to deal with flutter phenomena. Usage of multiple surfaces on the wing is well illustrated in [8]. In literature, numerous techniques from single input single output systems to frequency domain compensation methods for first bending mode attenuation are presented.

In the current research, the focus of active structural technique is to use multi-control surfaces of the wing to attenuate the buffet loads. The wing of advance commercial aircraft, X-DIA aeroelastic demonstrator built during European project named as Active Aeroelastic Aircraft Structure (3AS), is considered here [9]. As shown in figure (1), It has movable canards, vertical T-tail and forward swept aeroelastic wing. Each half of wing is equipped with four control surfaces, two are located at leading edge and two are located at trailing edge of the wing. They are named as leading edge inboard (LEI), leading edge outboard (LEO), trailing edge inboard (TEI) and trailing edge outboard (TEO).

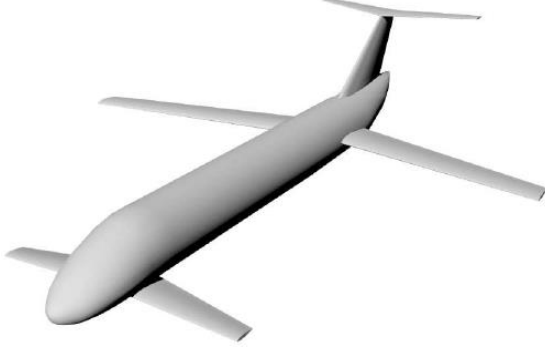


Figure 1: X-DIA Aeroelastic Demonstrator

The nomenclature of the aeroelastic wing is shown in figure (2), the wing is also equipped with four accelerometers and strain gauges to measure the real-time behaviour of the wing under dynamic loads and subsequently to be used in active control scheme. Two accelerometers are placed at the wing tip and two are placed at the midspan of the wing on either side of the elastic axis. Piezo-resistive pressure sensors attached on the surface of the wing provided the estimation of buffeting loads during the wind tunnel test campaign.

Analytical modelling of the wing has been realized in MSC/NASTRAN [9]. Numerical analysis performed on MSC/NASTRAN, provided the structural and aerodynamic coupling. MIMO (multi-input multi-output) state space model with 108 states has been developed by the in-house software MASSA. These states captured the true dynamics of the elastic modes of the wing. The control surfaces are driven by an active control law based on Static Output Feedback [7] controller to attenuate the buffet loads. Heuristic algorithms, provides the minimization of static output feedback controller by satisfying the Lyapunov equations criteria for stability. The task of attenuating the excited first bending and first torsion mode of the wing was numerically studied and it demonstrated the significant reduction in the power spectral density, frequency response and variance with active control system. Importance has also been given to the adaptability and robustness of the developed control scheme. To verify the robustness of the system, damping ratio and sensitivity of actuator and accelerometers are selected as the targets for the uncertainty in the system. Numerical and experimental investigation has been performed for the reliability of the system for the proposed technique of robustness.

The numerical study is followed by dedicated experimentation which took place in De Ponte Wind tunnel, Politecnico Di Milano-Department of Aerospace Science and Technology. Airbrake specifically manufactured for this task is installed ahead of the wing to produce buffet loads on the wing. Wind tunnel tests validated the numerical investigation with good accuracy performed on the X-DIA aeroelastic wing.

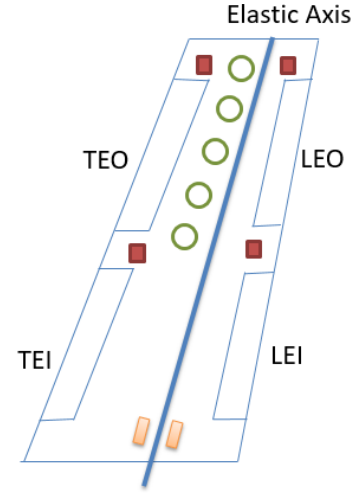


Figure 2: Aeroelastic Wing

II. NUMERICAL MODELLING

Commercially available software, MSC/NASTRAN is used to formulate the basis of numerical analyses such as modal test, modal frequency and dynamic aeroelastic analysis. Doublet Lattice method is used to simulate the aerodynamic effects on the wing. The formulated multi-input and multi-output state space model is validated with extracted modes from previous ground vibration testing of the wing. In house software built with cooperation of LEONARDO Company S.p.A., MASSA, based on MATLAB procedures, is used to couple the structural outputs and aerodynamic inputs to form the afore-mentioned state space model. Roger's technique is used to approximate the aerodynamic forces with minimal role of gust response matrix. Generalized aerodynamic response matrix with gust and aerodynamic response matrix is given by:

$$f = H_{am}(k, M_\infty) \cdot q + H_{ag}(k, M_\infty) \cdot \frac{V_g}{V_\infty} \quad (1)$$

The aeroelastic state space system have the form:

$$E_{ae} \dot{x}_{ae} = A_{ae} x_{ae} + B_{ae} f \quad (2)$$

Each structural degree of freedom is represented by 'q' generalized degree of freedom and 'r' virtual state. E_{ae} , A_{ae} , and B_{ae} are given by:

$$E_{ae} = \begin{bmatrix} M_{ae} & 0 & 0 \\ 0 & I & 0 \\ 0 & 0 & I \end{bmatrix} \quad A_{ae} = \begin{bmatrix} -C_{ae} & I & 0 \\ -K_{ae} & 0 & q_\infty C_a \\ (V_\infty/c)B_a & 0 & (V_\infty/c)C_a \end{bmatrix}$$

$$B_{ae} = \begin{bmatrix} 0 \\ I \\ 0 \end{bmatrix} \quad \dot{x}_{ae} = \begin{Bmatrix} \{\delta_i\} \\ q \\ \{\delta_{ir}\} \\ r \\ x_{ae} \end{Bmatrix} \quad (3)$$

Where:

$$M_{ac} = M_s - q_\infty (c/V_\infty)^2 D_2 \quad (4)$$

$$C_{ac} = C_s - q_\infty (c/V_\infty)^2 D_1 \quad (5)$$

$$K_{ac} = K_s - q_\infty D_0 \quad (6)$$

A_a , B_a and C_a can be calculated by solving the Roger's approximation for unsteady aerodynamic matrices. For more detailed insight, the reader is referred to [10]. The actuator dynamics can be modelled by the form $\{\delta_i\} = [H_\delta] \{\delta_{c,i}\}$, it can be casted in the aeroelastic model to form the complete aeroservoelastic system. The completed state space form had eight outputs, four accelerations and four control surface rotations, while the model had 13 inputs, 5 inputs for piezo resistive pressure sensors attached on the surface of the wings, 4 inputs for actuators corresponding to four control surfaces on the wing and 4 inputs for the forces at the points of accelerometers.

In Table (1), the first five elastic modes are presented with the respective frequencies, figure (3) and figure (4) show the modal shape of the first bending mode and of the first torsion mode, respectively.

TABLE I
MODAL PROPERTIES

Mode no.	Frequency, Hz	Mode shape
1	9.390	1 st bending mode
2	11.13	1 st in plane bending mode
3	24.63	1 st torsion mode
4	39.84	1 st TEO bending mode
5	47.06	2 nd bending mode

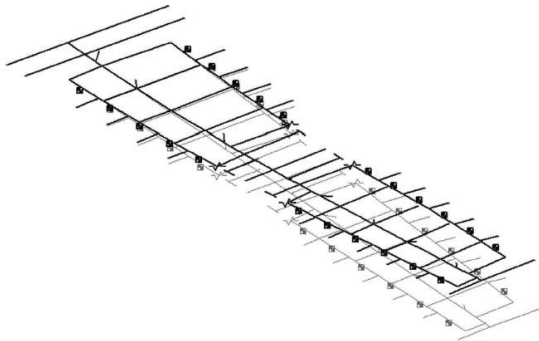


Figure 3: First bending Mode (9.390Hz)

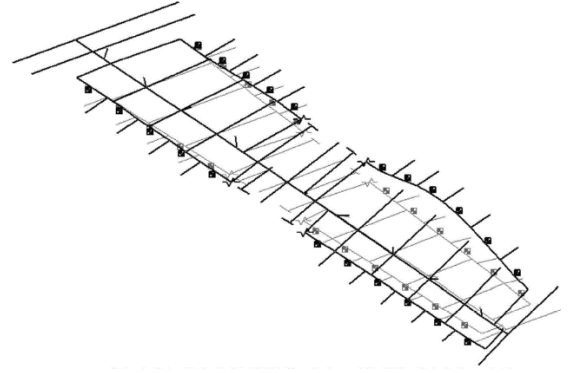


Figure 4: First Torsion Mode (24.630Hz)

Numerical flutter test is shown in figure (5), it revealed that the zero damping for the first torsion mode is achieved around 60 m/s. In the context of these results, the state space model has been prepared for variable velocities from 20 m/s to 40 m/s, later the experimentation is conducted at the prescribed velocities. Second order dynamics of actuator is selected to represent each actuation system on the wing, with addition of the states for pseudo integrators in the plant, the final design contains 124 states for the plant.

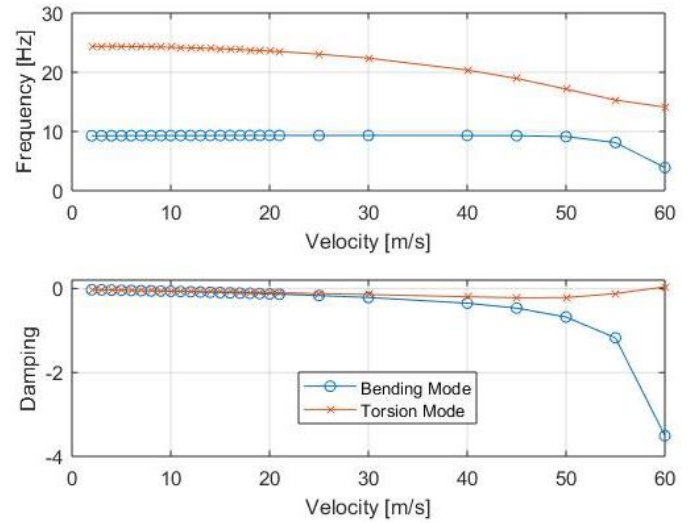


Figure 5: V-g, V-f Graph

III. ACTIVE CONTROL SCHEME

The four outputs from accelerometers are used as feedback to the actuators, forms the foundation for the implementation of active control scheme to suppress the structural vibrations through changing the camber of the wing by deflecting the control surfaces, which in return redistribute the aerodynamic loads to cater the vibrations produced in the wing. The outputs from accelerometers are arithmetically changed to fit the demand of modal control. The standard practice followed in modal control is to isolate the signals by forming suitable combinations as reported in [10].

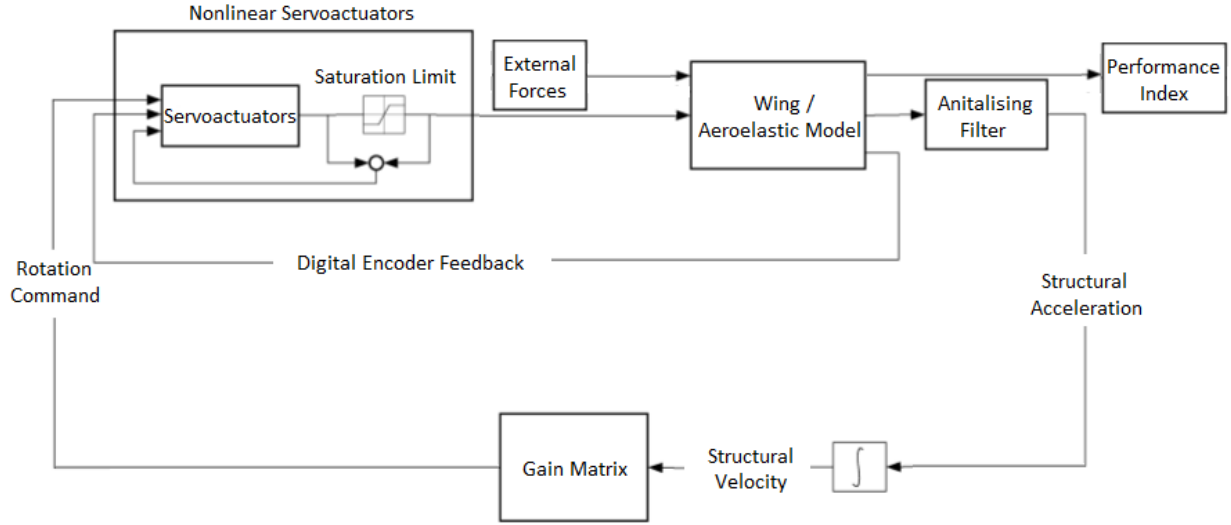


Figure 6: Control Scheme

In the current research, more conservative idea is used with more weight given to the accelerometer farthest from elastic axis for bending signal and equal weighting to accelerometers on either side of the elastic axis for torsional signal. It can be given in the matrix form as:

$$\begin{Bmatrix} \text{Ben} \\ \text{Tor} \end{Bmatrix} = \begin{bmatrix} 0 & 1 \\ 1 & -1 \end{bmatrix} \begin{Bmatrix} \text{Acc}_{\text{LEI/O}} \\ \text{Acc}_{\text{TEI/O}} \end{Bmatrix} \quad (7)$$

It is possible to extract the velocities from the accelerometers through pseudo integrators given by the following relation:

$$v(s) = \frac{\omega_f^2 s}{s^2 + 2\xi_f \omega_f s + \omega_f^2} a(s) \quad (8)$$

The numerical analysis showed that the attenuation demonstrated for only bending signal is most suitable for first bending mode, while the torsion signal is better in the torsional mode. The formulated aeroservoelastic state space model act as a linear time invariant system (LTI) for active control scheme. It can be modified for the static output feedback and is given by the following form:

$$\begin{aligned} \dot{x} &= Ax + B_u u + B_d d \\ y &= C_y x + D_{yu} u + D_{yd} d + n \\ z &= C_z x + D_{zu} u + D_{zd} d \end{aligned} \quad (9)$$

Where, $x \in \mathbb{R}^n$ represents state vector, $u \in \mathbb{R}^{m_u}$ represents controlled input, $d \in \mathbb{R}^{m_d}$ represents turbulent input with appropriate shape filtering, $z \in \mathbb{R}^{l_z}$ represents performance index. The gain matrix given by $G' = (I + GD_{yu})^{-1}G$, can be formed by the output feedback of the form $u = -G'y$, subsequently the close loop system can be calculated by

substituting the output feedback in equation (9). The formulated system can be heuristically minimized by defining quadratic objective function based on performance index and input to the system. The feasibility of the solution is provided by Lyapunov equations with also indirectly checking observability and controllability of the system. The minimization in the feasible region is obtained by second order quadratic formulation of the objective function by using the Levenberg-Marquardt (LM) algorithm. It shifts between Gradient descent and Newton's method depending upon the proximity to the solution. It minimizes the objective function by $H(g) \in \mathbb{R}^{n \times n}$ of the form:

$$H = J^T J + \lambda^2 (J^T J) \quad (10)$$

Iterative procedure given by $g^{k+1} = g^k - H^{-1} \times \nabla J$, reduces the given objective function, where 'J' defines the Jacobian of the objective function. The procedure is well explained in [11]. The control scheme architecture adopted for this case is shown in figure (6), each actuator has been provided with separate PID_2 controller, with an additional derivative term to compensate for faster step response and to meet the bandwidth criteria. The saturation of the actuators has been controlled by the constant weighting functions associated with objective function as suggested by the author [13]. The optimization of the system is accomplished by allowing the user to readily change the outputs and inputs to extract the desired results. This strategy is opted by keeping in view the large quantity of instrumentation associated with the wing, i.e. choice between four actuators and four accelerometers. Nonlinearity in the actuation system is dealt by adding a dead zone in the PID_2 . Each PID_2 controller is also equipped with anti-windup scheme. Figure (7), shows the comparison of outboard edges with inboard edges for inactive and active control scheme.

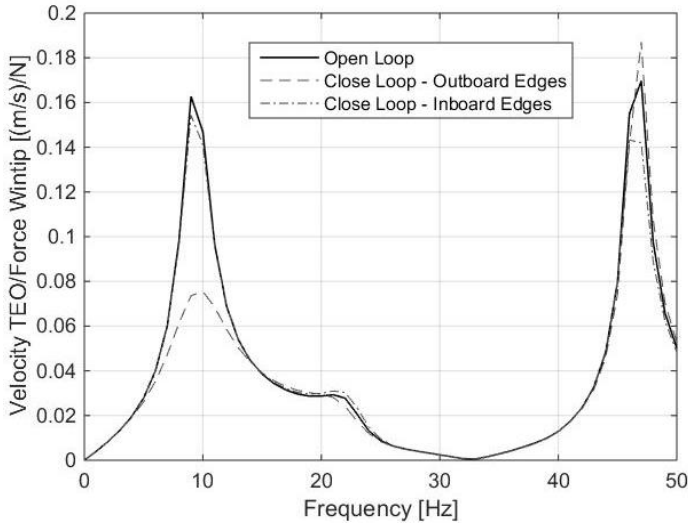


Figure 7: Numerical Frequency Response

The data is extracted from accelerometer located at the trailing edge for different actuator (control surface) / sensor (accelerometer). Figure (8), provides the numerical frequency response of trailing edges, it predicted the open loop response of developed state space model with external disturbances, close loop response showed not only attenuated responses but highly damped responses as well in the first bending and torsion mode.

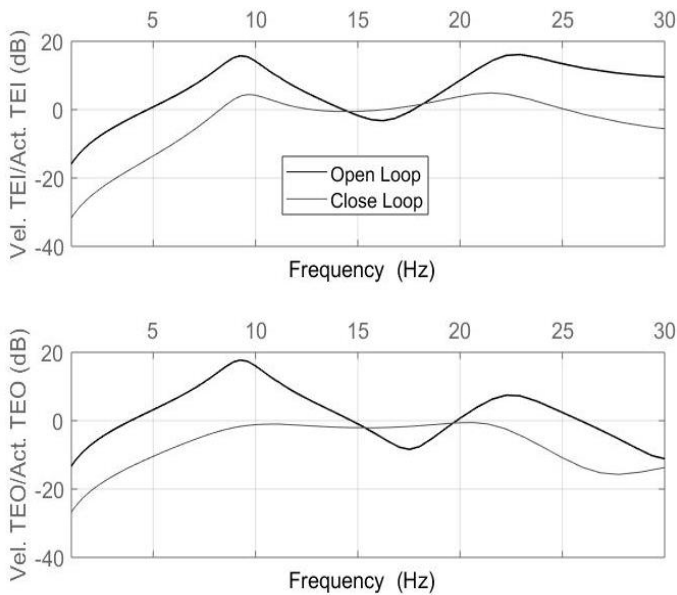


Figure 8: Numerical Frequency response of trailing edges

IV. WIND TUNNEL TESTING

Active control scheme on the X-DIA wing is experimentally tested in De Ponte wind tunnel at Politecnico di Milano-Department of Aerospace Sciences and Technology. The wind tunnel has been equipped with airbrake in the horizontal direction. The wing has been attached in the wake of the airbrake in the middle of the test section, which has dimensions of $1.5 \times 1 \text{ m}^2$. Figure (9),

shows the view of the test section with attached wing and airbrake in the operating position. Pitching angles of both wing and airbrake can be adjusted as per the requirement. The data from accelerometers is conditioned by antialiasing filters.



Figure 9: Experimental Setup - Test Section

A setup had been prepared with input (NI 6036) and output (NI 6713) boards driven by open source Comedi [10]. The actuator motors are equipped with planetary gears having gear ratio of 88 and 22 for leading edges and trailing edges respectively. The designed PID_2 controller along with actuators permitted to have the frequency bandwidth of 30Hz. Hardware is configured via software by the help of QRTAILAB GUI, running under RTAI environment compatible with Linux operating system [12]. The test section speed is set at 30 m/s, almost half of the flutter speed predicted during numerical investigation phase. Tests for robustness are performed at 20m/s due to safety issues associated with the instrumentation and structure of the wing.

Figure (10), shows the experimental results for active control scheme, frequency response is presented to show the attenuation achieved by the active control scheme. Each curve represents the response for each of the four actuators with respect to corresponding accelerometer. The attenuations for the first bending mode and first torsion modes are remarkable. The comparison is also drawn for the performance of outer strip of the wing (combination of TEO and LEO) and inner strip (combination of TEI and LEI) of the wing, see figure (11). Power spectral density demonstrated that outboard strips are better in attenuating

first bending loads whereas inboard strips are better in the first torsional mode.

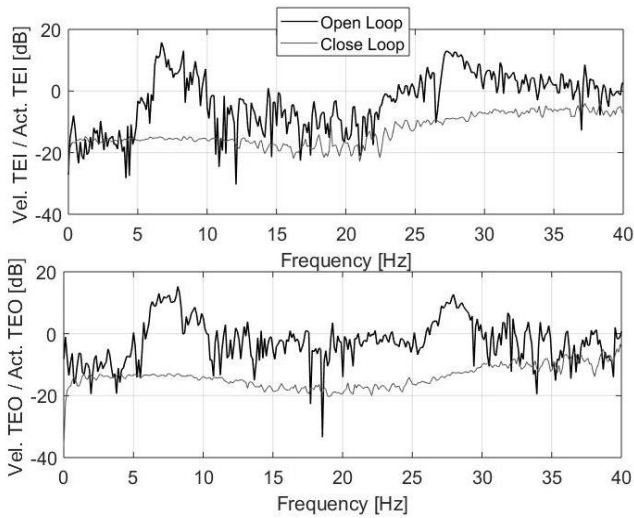


Figure 10: Experimental Frequency response of Trailing edges

Figure (12-14), shows the experimental checks for the instrumentation involved in the wind tunnel test on the wing. Figure (12), shows the command generated by the active control scheme and consequently the action of actuator with respect to the command. It is apparent that the actuator followed the command with good precision with a small phase delay as suggested by [10]. Figure (13), demonstrated the 28.73 percent reduction in variance of the acceleration for active control scheme. Figure (14), showed that the control surfaces operated within the saturation range (± 10 volts) of the motors during active control systems.

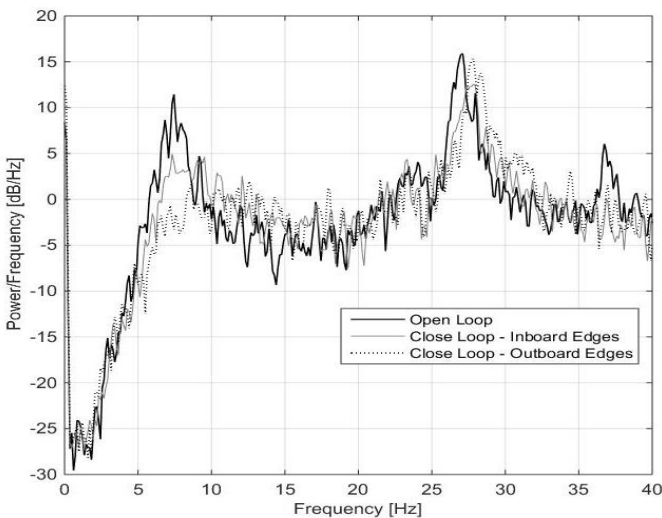


Figure 11: Experimental Power Spectral Density comparison for Inner and Outer strips

Average work done by each actuator is extracted from variance of control surface movement. TEO performs more work as compared to the other surfaces. LEO performs the least amount of work to attenuate the structural vibration.

All the results demonstrated that the instrumentation is working well within the safety bounds.

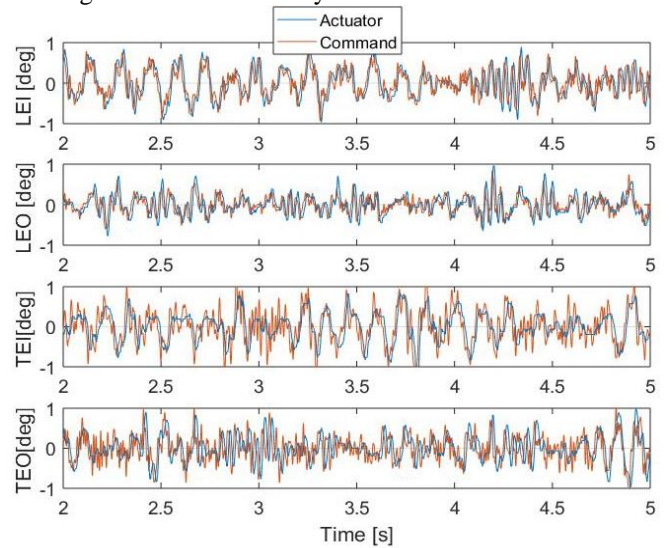


Figure 12: Time histories of Command and Actuator

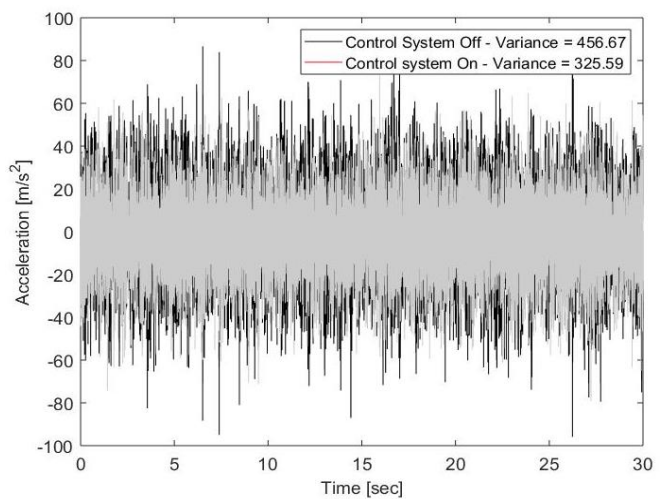


Figure 13: Time history of Acceleration (Variance)

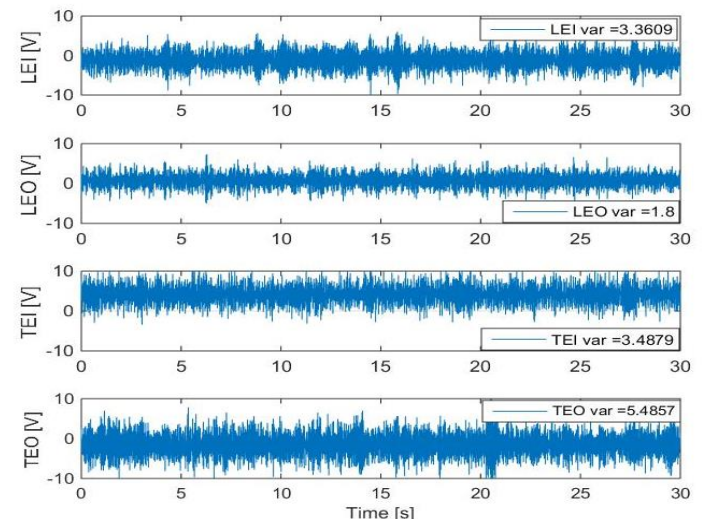


Figure 14: Time histories of control voltages

V. PARAMETRIC UNCERTAINTY ANALYSIS

The afore-mentioned control optimization strategy is investigated for uncertainties introduced in the instrumentation of the wing. The numerical model is intentionally made uncertain with the help of parametric uncertainties introduced through built-in MATLAB functions by augmenting sensitivity of the accelerometers and damping ratio of the actuators. The outputs from the accelerometers are incorporated with efficiency factor. While, the damping ratio is augmented in second order dynamics of the actuators. Several samples are obtained for uncertainty in the actuation system. This is shown in the figure (15) in terms of frequency response, for these cases the control strategy has been optimized. With percentage of uncertainty defined, the algorithm calculated the set of gains for static output feedback controller. The increase in uncertainty showed the gradual decrease in the performance of the active control system. The numerical analysis shows that the gain margin and phase margin is decreased but overall the system remains in the stable region. Figure (16), shows the effect of uncertainty on the TEO for the first bending mode, with attenuation approaching zero as uncertainty reaches 75% in the TEO.

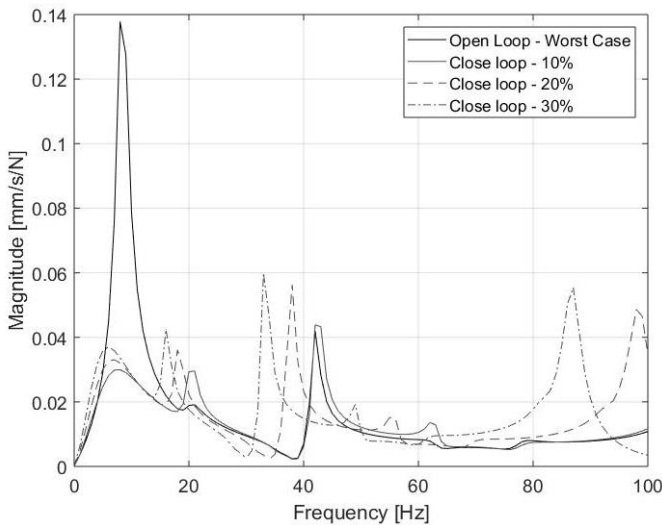


Figure 15: Trailing edge Uncertainty

Figure (17), shows the numerical results for uncertainty in the output feedback of the system. Intuitively, under maximum uncertainty the system behaves like open loop system, which is demonstrated in the figure, the attenuation is diminishing as the uncertainty in output feedback system is increased. The experimental results for the active control systems for uncertainty in the actuator and output feedback (Accelerometer) is presented in figure (18,19). Only the closed loop responses are presented for the comparison.

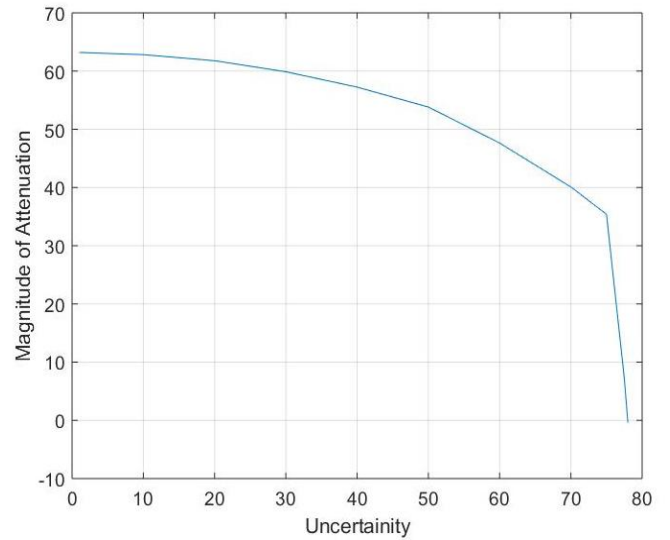


Figure 16: TEO Sensitivity to Uncertainty

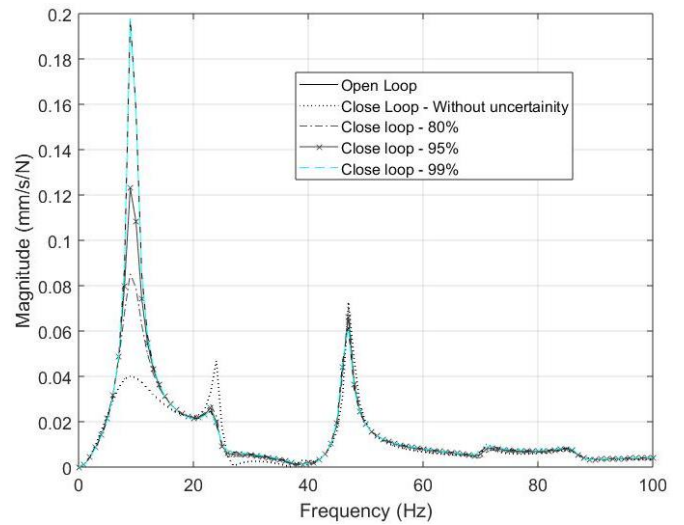


Figure 17: Uncertainty in The Output Feedback

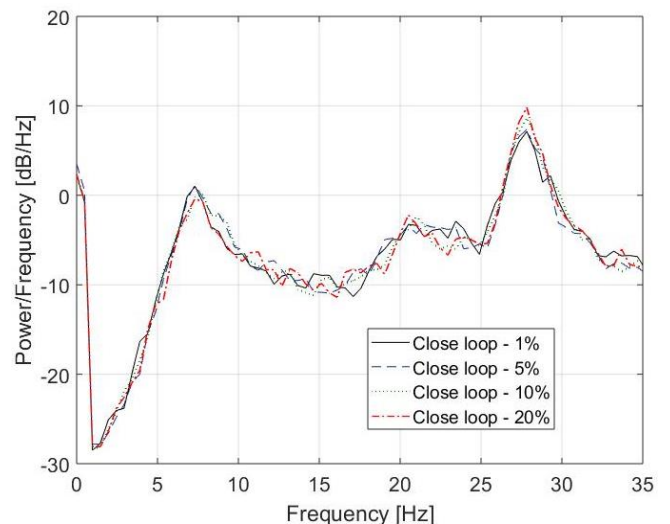


Figure 18: Experimental - Trailing Edge Sensitivity

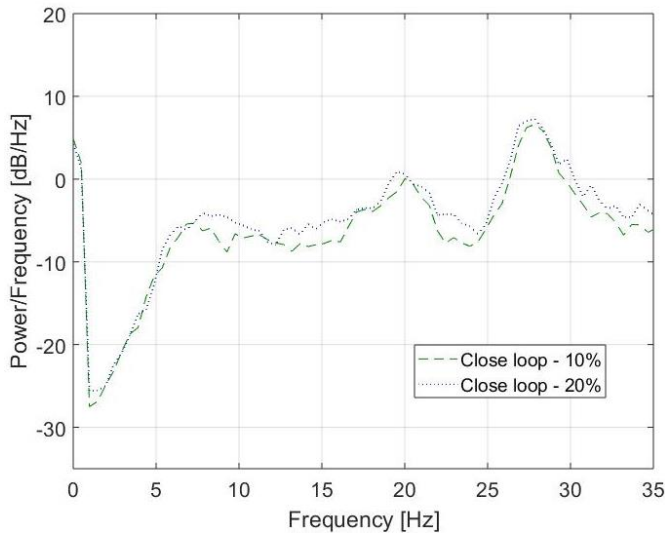


Figure 19: Experimental - Uncertainty in the Accelerometer

The high amount of uncertainty chosen for numerical analysis is not implemented due to the risk of catastrophic failure. However, uncertainty up till 20 percent is experimentally tested. It can be clearly observed that the performance of the system is deteriorating especially in the range of torsional mode frequency.

VI. CONCLUSIONS

This paper has presented a control scheme based on static output feedback controller with minimization of the objective function achieved by the Levenberg-Marquardt algorithm, based on second order quadratic formulation of the objective function. The target of this research was to attenuate the amplitude of the vibrations in the first bending and first torsion mode with the help of individual actuator and combination of actuators. In the first phase, the model was investigated numerically, which demonstrated the ability of the system to attenuate the vibrations in the known and in the uncertain conditions as well with a compromise on performance. Surface of the wing was equipped with pressure sensors to estimate the buffet loads produced by the airbrake in the wind tunnel. Airbrake was installed to replicate the vortices which induces buffet loads.

The results demonstrated that the actuators operated well under the limit of saturation of the motors of 10V. It was also showed experimentally that the active control signal obeyed the command with high precision. The attenuation achieved for all the control surfaces was remarkable. Outboard edges were quite beneficial as compared to inboard edges for attenuation of structural vibrations. Variance of the TEO accelerometer was decreased to 28.73 % for active control system. Robustness of the optimization algorithm ensured the robust system under uncertainties in the instrumentation of the wing. The performance of the system was inversely proportional to the uncertainty introduced in the system.

ACKNOWLEDGMENT

The authors would like to thank Donato Grassi for his help throughout the wind tunnel test campaign.

REFERENCES

- [1] R. M. Hauch, J. H. Jacobs, C. Dima, and K. Ravindra, "Reduction of Vertical Tail Buffet Response using Active Control", *Journal of Aircraft*, Vol. 33, No. 3, 1996, pp. 617-622.
- [2] P. Seiler, G. J. Balas and A. Packard, "Linear Parameter Varying Control for the X-53 Active Aeroelastic Wing", In *AIAA Atmospheric Flight Mechanics Conference*, 2011, Portland, United States.
- [3] Y. H. Zhao and H. Y. Hu, "Active Control of Vertical Tail Buffeting by Piezoelectric Actuators", *Journal of Aircraft*, Vol. 46, No. 4, 2009, pp. 1167-1175.
- [4] D. E. Bean, D. I. Greenwell, N. J. Wood, "Vortex Control Technique for the Attenuation of fin Buffet", *Journal of Aircraft*, Vol. 30, No. 6, 1993, pp. 847-853.
- [5] K. B. Lazarus, E. Sarmaa and G. S. Agnes, "Active Smart Material System for Buffet Load Alleviation", *Proceedings of SPIE: The International Society for Optical Engineering*, Vol. 2447, 1995, pp. 179-192.
- [6] F. Nitzsche, D. G. Zimeik, K. Langille, "Active Control of Vertical Fin Buffeting with Aerodynamic Control Surface and Strain Actuation", *AIAA paper*, 1997-1386, 1997.
- [7] F. Fonte, S. Ricci and P. Mantegazza, "Gust Load Alleviation for a Regional Aircraft Through a Static Output Feedback", *Journal of Aircraft*, Vol. 52, No. 5, 2015, pp. 1559-1574.
- [8] D. J. Lucia, "The Sensocraft Configurations: A Non-Linear Aeroservoelastic Challenge for Aviation", *Proceedings of the 46th AIAA/ASME/ASCE/AHS/ASC Structures, Structural Dynamics and Materials Conference*, AIAA, 2005, Reston, VA.
- [9] J. Malecek, J. Cecrdle, A. Scotti, S. Ricci, F. Kiessling and T. Klimmek, "Dynamic Response Analysis and Experimental Validation of the X-DIA Demonstrator Component Model", *Proceedings of the IFASD International Forum on Aeroelasticity, International Forum on Aeroelasticity and Structural Dynamics*, 2005, Munich, Germany.
- [10] A. De Gaspari, S. Ricci, L. Riccobene and A. Scotti, "Active Aeroelastic Control Over a Multisurface Wing: Modeling and Wind-Tunnel Testing", *AIAA Journal*, Vol. 47, No. 9, 2009, pp. 1995-2009.
- [11] S. Malik, L. Riccobene, S. Ricci and D. Monti, "Development of a Buffet Load Mitigation System based on Multi-Surface Control", *International Forum on Aeroelasticity and Structural Dynamics*, IFASD June 2017, Como, Italy.
- [12] L. Dozio and P. Mantegazza, "Real Time Distributed Control Systems Using RTAP", *Proceedings of International Symposium on Object-Oriented Real-Time Distributed Computing*, ISORC, Hakodate, Japan, 2003, pp. 11-18.
- [13] E. H. Dowell, "A Modern Course in Aeroelasticity, Solid Mechanics and its Applications", 2015, DOI 10.1007/978-3-319-09453-3_12.